NDCX-II Experimental Plans and Target Simulations

J. J. Barnard[1], R. M. More[1,2], P. A. Ni[2], A. Friedman[1], E. Henestroza[2], I. Kaganovich[3], A. Koniges[2], J. W. Kwan[2], W. Liu[2], A. Ng[4], B.G. Logan[2], E. Startsev[3], M. Terry[1], A. Yuen[2]

1. Lawrence Livermore National Laboratory
2. Lawrence Berkeley National Laboratory
3. Princeton Plasma Physics Laboratory
4. University of British Columbia

West Coast High Energy Density Science Cooperative Meeting

Berkeley and Palo Alto, California

January 22-23, 2013

The Heavy Ion Fusion Science Virtual National Laboratory

* This work was performed under the auspices of the U.S. Department of Energy by Lawrence Livermore National Security, LLC, Lawrence Livermore National Laboratory under Contract DE-AC52-07NA27344, by LBNL under Contract DE-AC02-05CH11231, and by PPPL under Contract DE-AC02-76CH03073.

Outline of talk: NDCX-II target physics plans and simulations

NDCX-II physics experiments:

1. Heavy ion fusion beam physics (discussed by Alex)

2. HEDLP physics

   -- Target coupling/ion driven hydrodynamics
      Rarefaction waves
      Shock waves

   -- Ion dE/dX in heated matter

   -- Material properties (such as conductivity) in heated matter

Original strategy: maximize uniformity and efficiency by placing center of foil at Bragg peak

In simplest example, target is a foil of solid or “foam” metal

Fractional energy loss can be high and uniformity also high if operate at Bragg peak (L. R. Grisham, Physics of Plasmas, **11**, 5727 (2004).)

Example: Ne

Energy loss rate

$$-\frac{1}{Z^2}\frac{dE}{dX}$$

(MeV/mg cm^2)

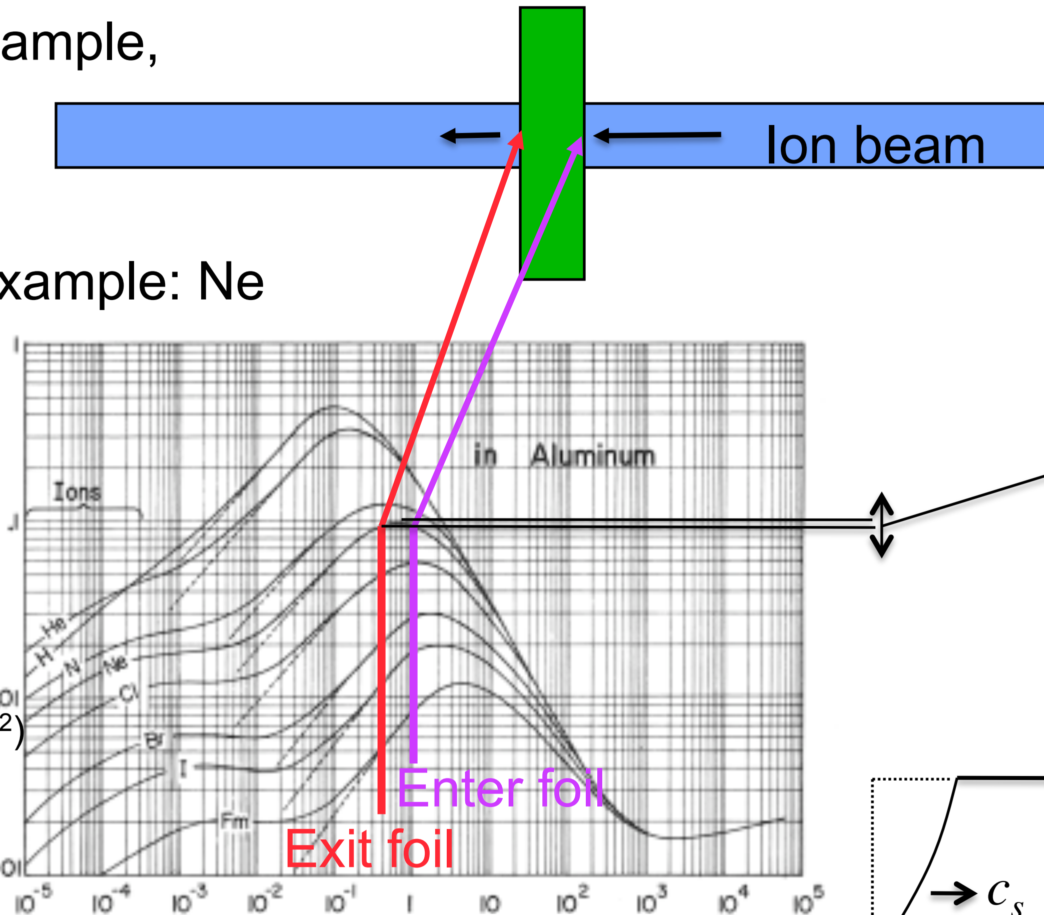

$\Delta dE/dX \propto \Delta T$

Energy/Ion mass (MeV/amu)

(dEdX figure from L.C Northcliffe and R.F.Schilling, Nuclear Data Tables, A7, 233 (1970))

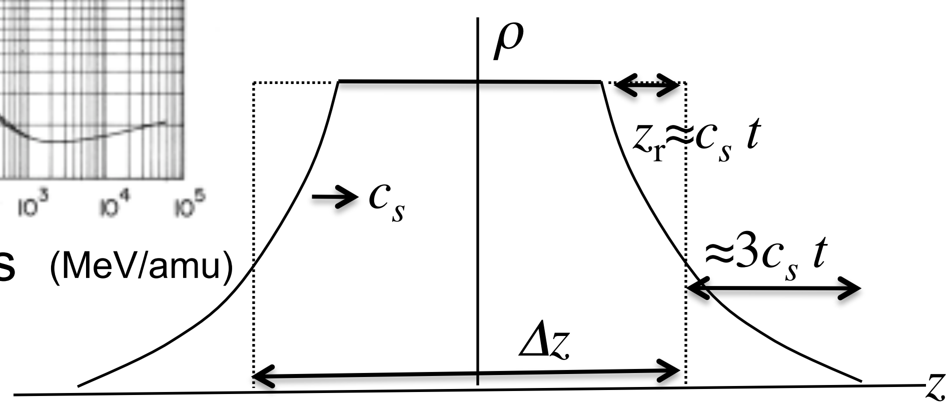

The initial configuration of NDCX-II has an ion energy of 1.2 MeV; a second stage is envisioned with an ion energy of 3.1 MeV

	Initial configuration	Stage II (~2015?)
	27 periods/12 active-cells	37 periods/21 active-cells
Ion species	Li^{+}: A=7	Li^{+}: A=7
Total charge in final pulse	30 -50 nC	30 – 50 nC
Ion kinetic energy	1.2 MeV	3.1 MeV
Focal radius (containing 50% of beam)	0.6 mm	0.7 – 0.5 mm
Bunch duration (FWHM)	0.9 – 0.6 ns	0.6 – 0.2 ns
Peak current	36 A	50 – 250 A
Peak fluence (time integrated)	~8 - 10 J/cm^2	~28 J/cm^2
Peak target temperature	~ 1 – 1.5 eV	~ 2 – 3 eV
Peak target pressure	0.05 – 0.2 MBar	0.2 – 0.8 MBar

* Estimates of ideal performance are from (r,z) Warp runs (no misalignments), and assume uniform 1 mA/cm^2 emission of ions, no timing or voltage jitter in acceleration pulses, no jitter in solenoid excitation, and perfect beam neutralization.

Bragg peak is at 1.9 MeV for Li on Al (so ~3 MeV desirable) At 1.2 MeV Li is below peak for most materials

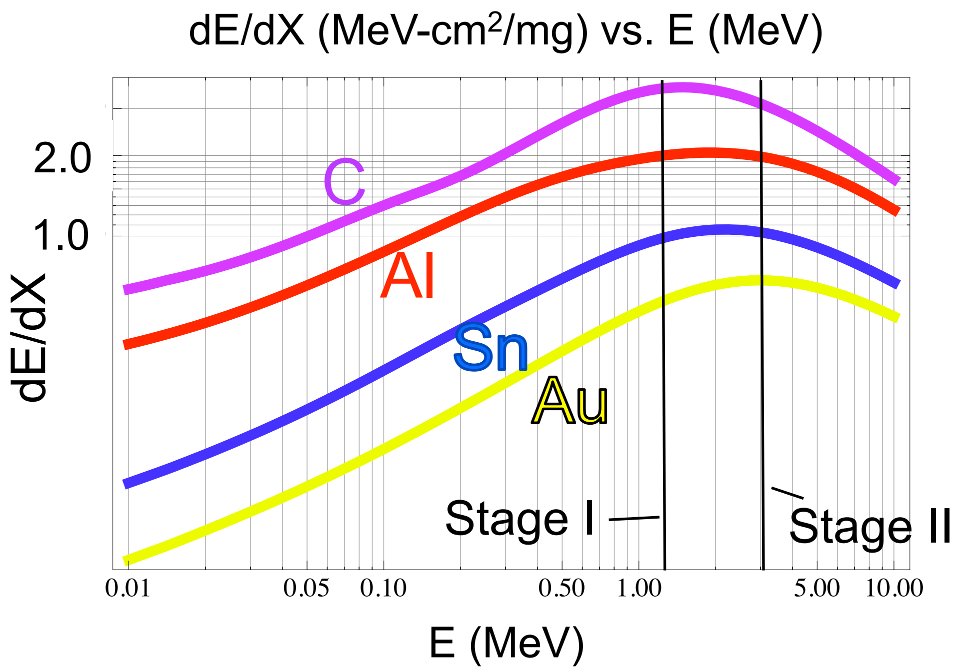

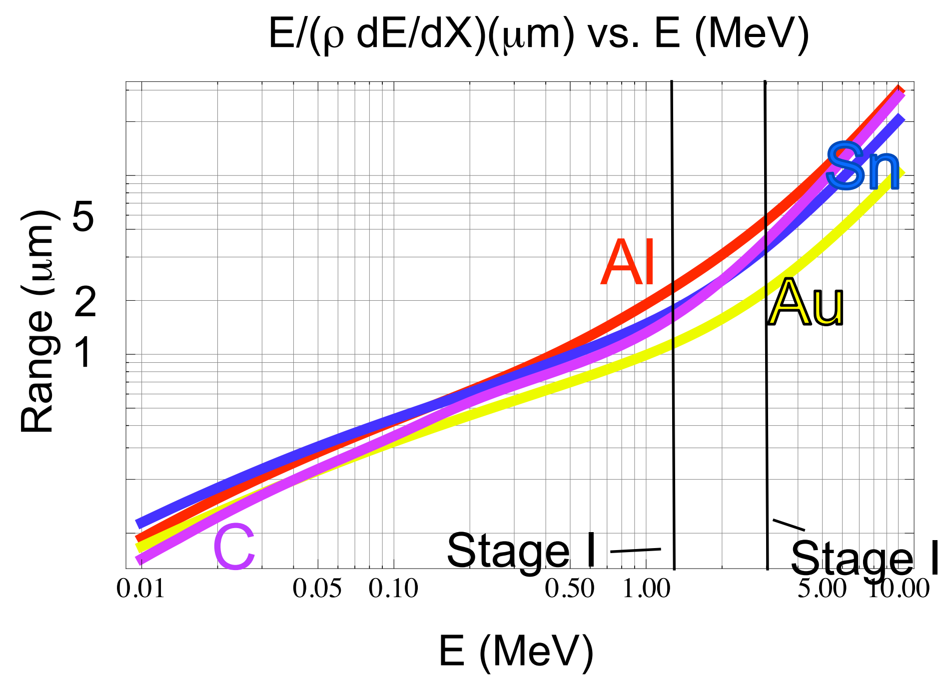

Bragg peak energies, Li on:

C	1.5 MeV
Al	1.9 MeV
Sn	2.0 MeV
Au	3.0 MeV

In the WDM regime, equations of state vary between models

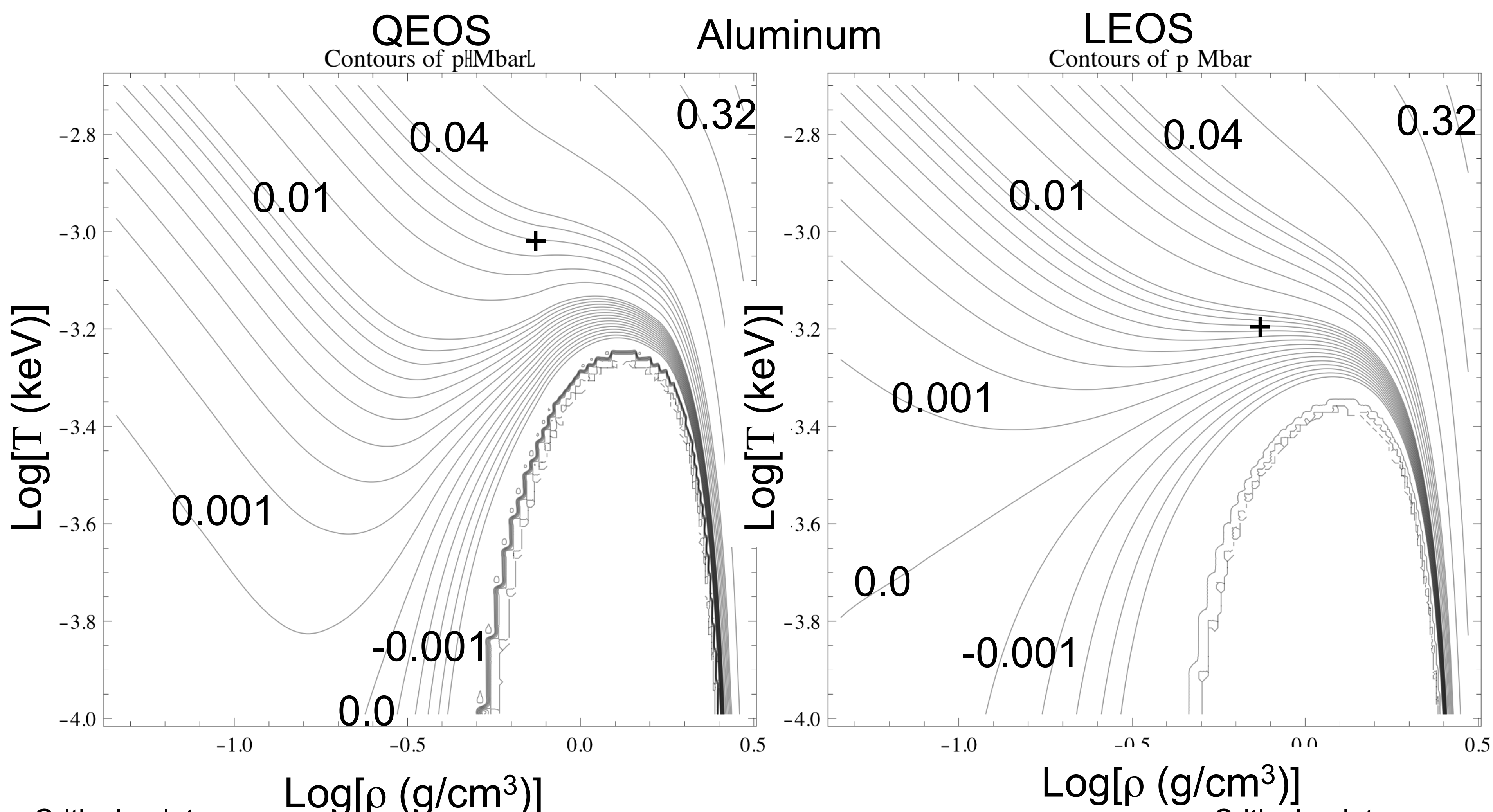

Critical point:
p=0.029 MBar
ρ=0.78 g/cm^3
T=0.945 eV

Theories and experiments place critical point between 5500 K and 12000 K (0.5 eV and 1.0 eV)

Critical point:
p=0.0065 MBar
ρ=0.70 g/cm^3
T=0.633 eV

At 1.2 MeV ion energy, with 1 μ thick targets, there is a significant difference in target response depending on EOS

Assumed fluence:
12 J/cm^2; 1.2 MeV
Li beam on Al
target (1 ns)

density

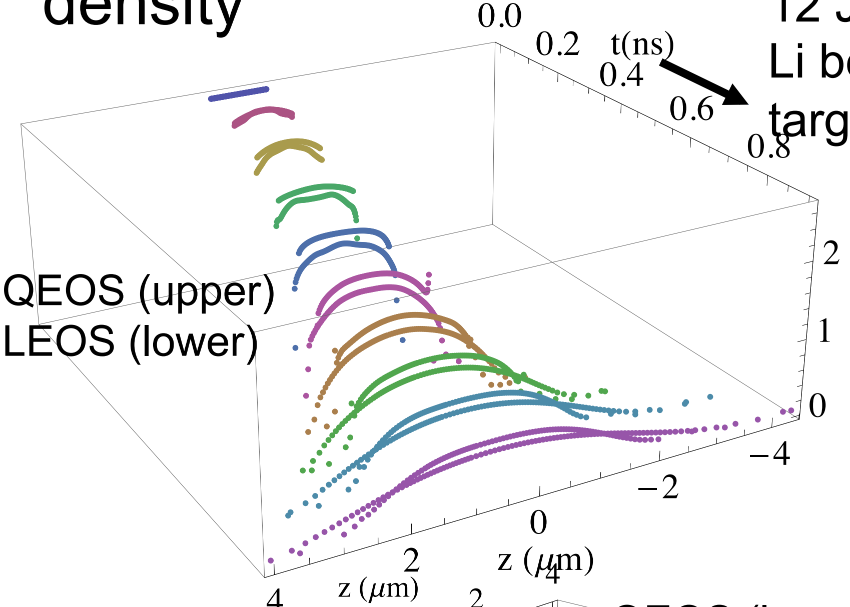

QEOS (upper)
LEOS (lower)

temperature

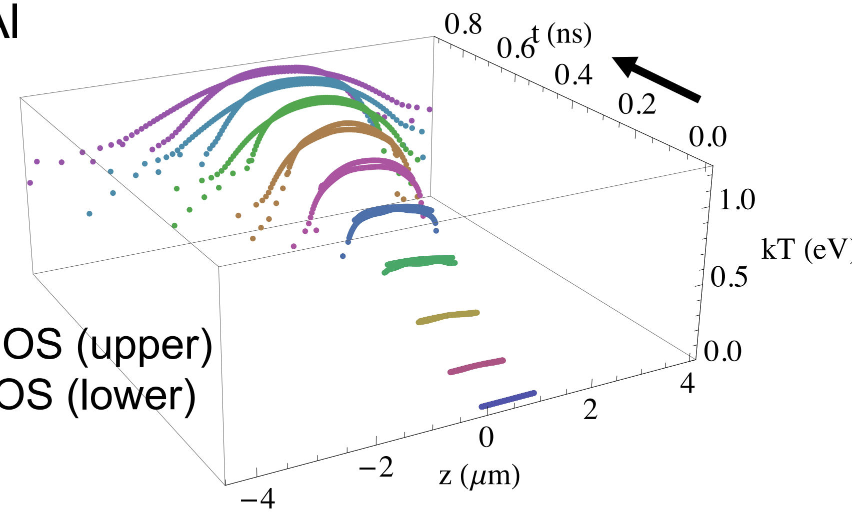

QEOS (upper)
LEOS (lower)

pressure

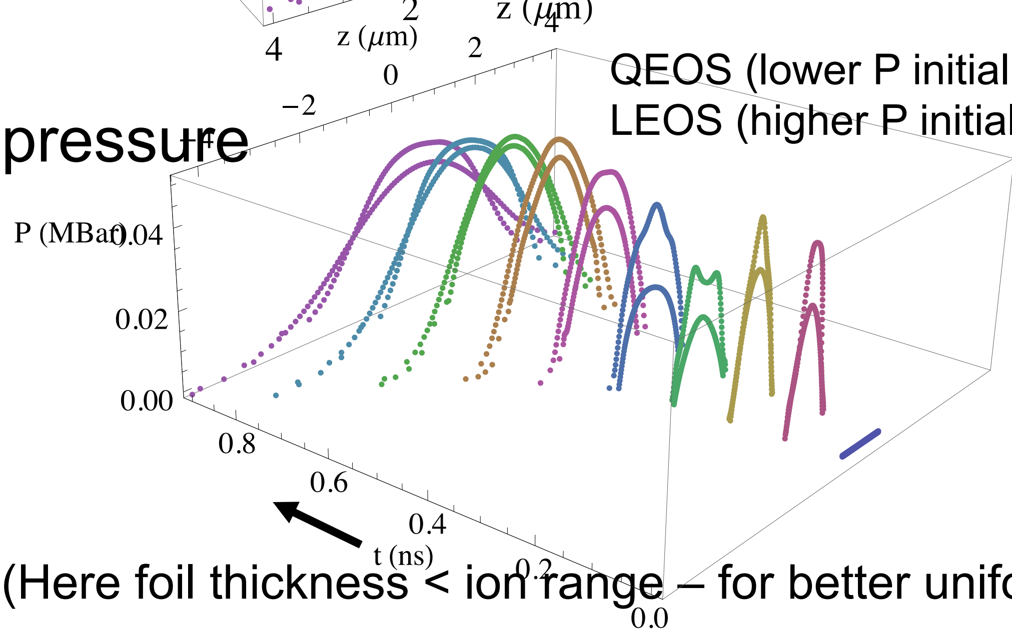

QEOS (lower P initially)
LEOS (higher P initially)

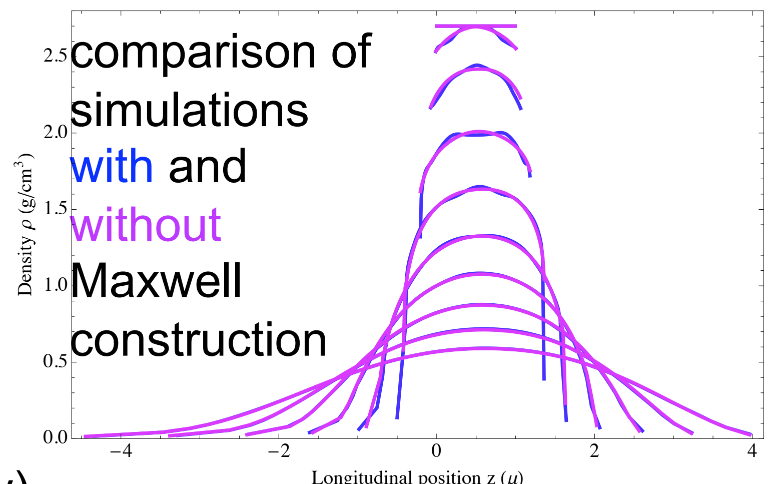

comparison of simulations with and without Maxwell construction

(Here foil thickness < ion range – for better uniformity)

Diagnostics for temperature, velocity and density will be compared to simulated diagnostics and depend on EOS

Pyrometry

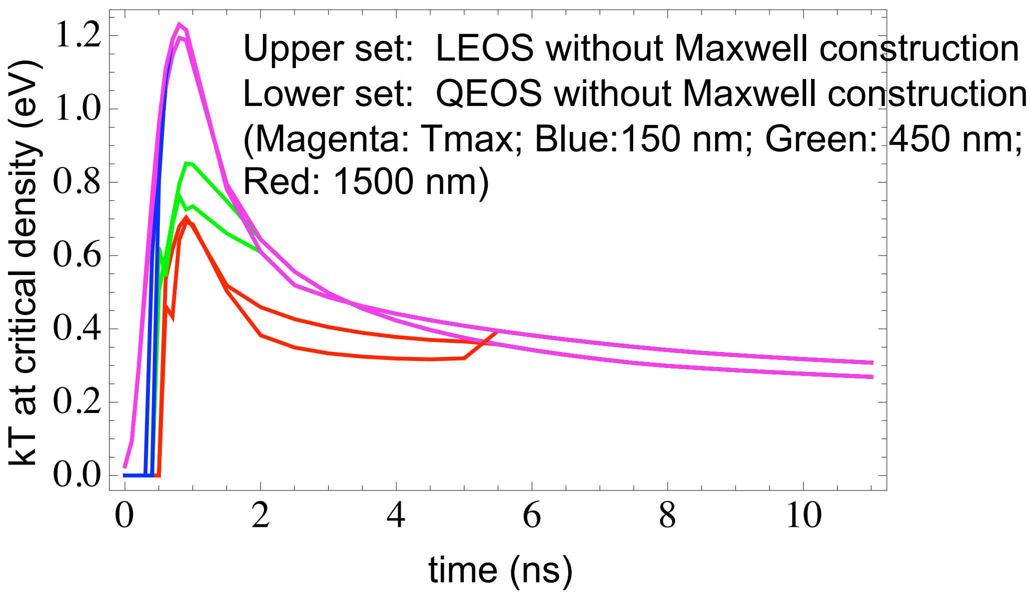

VISAR

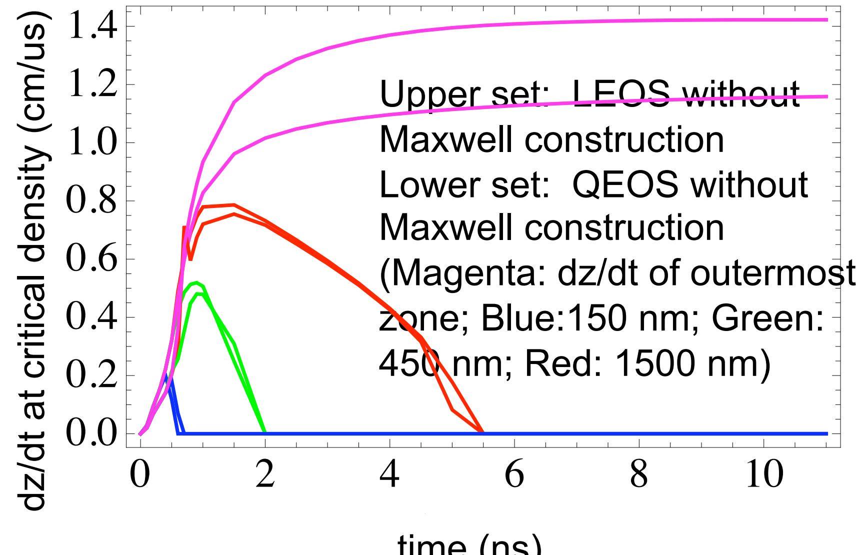

X-ray imaging of density profile (lower, shown at 10 different snapshots) can distinguish between EOS

X-pinch

Multi-frequency (upper left) and multi-angle pyrometry measurements, together with multi-frequency Visar measurements (upper right) can distinguish between EOS candidates.

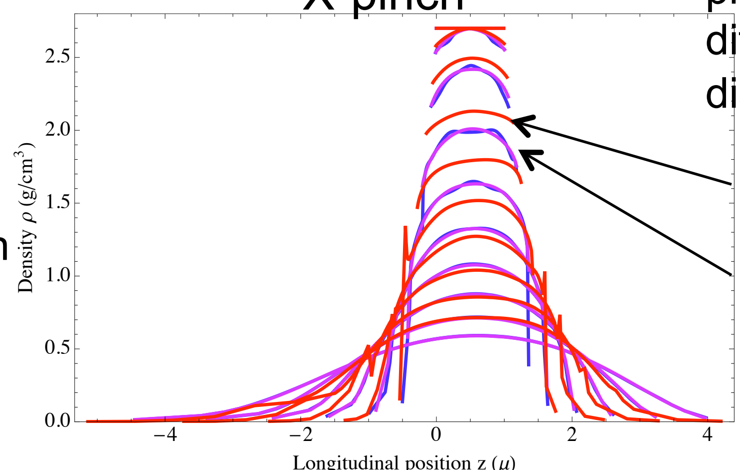

Upper (in each pair): QEOS without Maxwell construction
Lower (in each pair): LEOS without and **with** Maxwell construction

(Snapshots separated by 0.1 ns

(1.2 MeV, 12 J/cm^2, 1 ns Li^+ ion beam on Al target)

When foils are thicker than the ion range, shocks may form and be measured

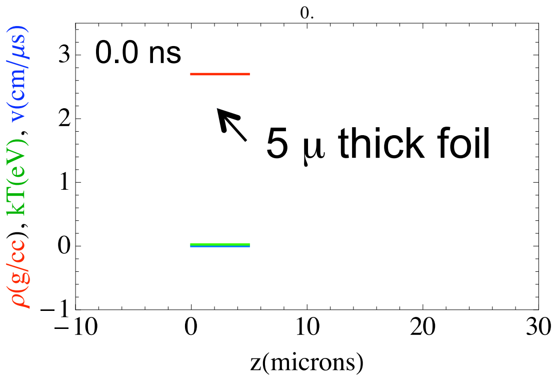

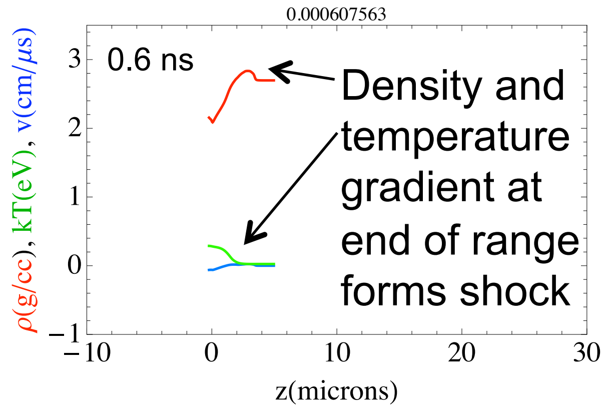

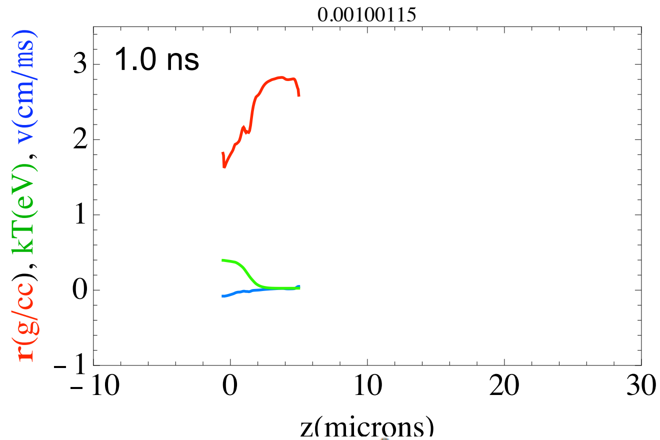

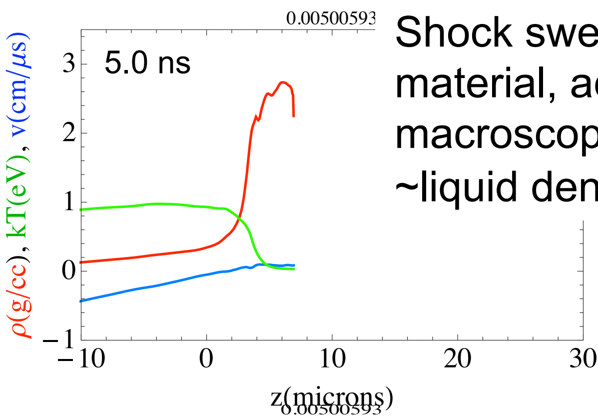

Shock sweeps through material, accelerating macroscopic slab at ~liquid density

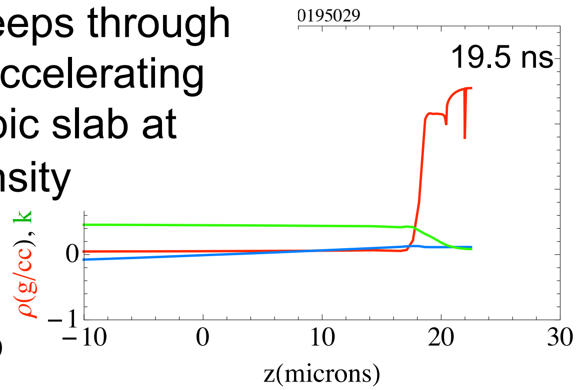

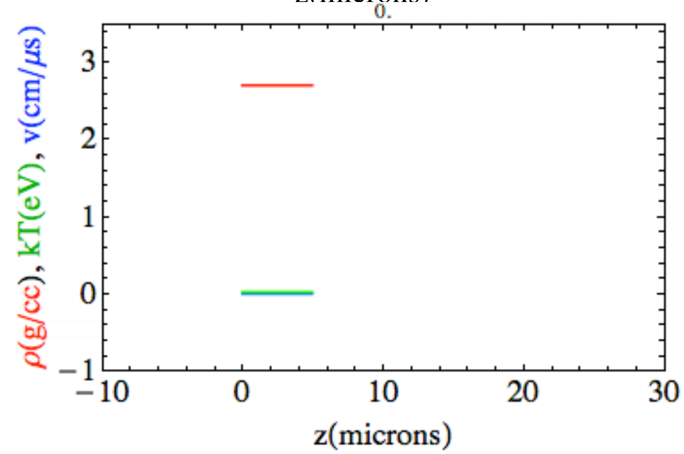

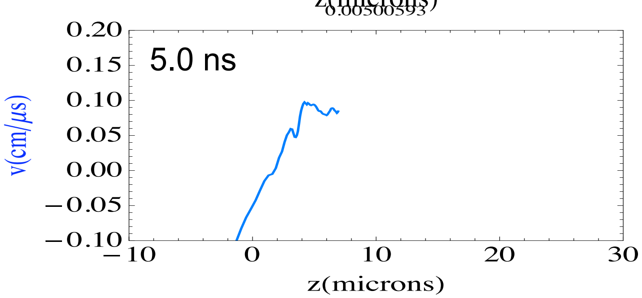

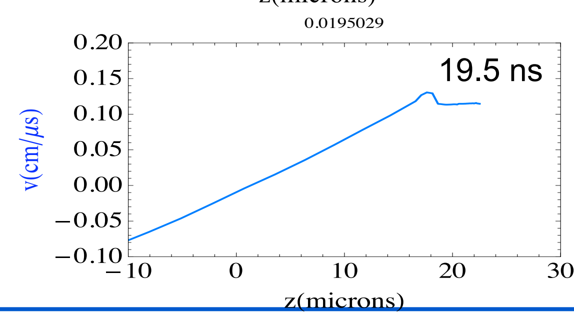

Shocks in solids are limited to small density enhancements, however, shocks in foams can produce large density contrasts.

Shock strength depends on energy profile but also depends on intensity profile (and thus on how the beam focused in z, r)

Shock strength maximization with ion beams involves determining optimum velocity tilt and focusing angle:

Large velocity tilt gives:

- larger range variation (larger variation in penetration depth)
- shorter pulse duration
- larger chromatic variations (*i.e.* larger spot radii at high velocity ends)

Large focusing angle:

- smaller radius for midpulse of beam
- larger chromatic variations (*i.e.* larger spot radii at high velocity ends)

For WDM (shockless) applications, requirements of short pulse and maximum energy density lead to large velocity tilt and optimum focusing angle

For applications that create a shock, placing energy behind shock implies optimum may shift to longer pulses and smaller focusing angles

Tampers (that can be used in HI direct drive targets) can create additional shocks that can merge with the primary (M. Terry)

NDCX-II experimental scenario:

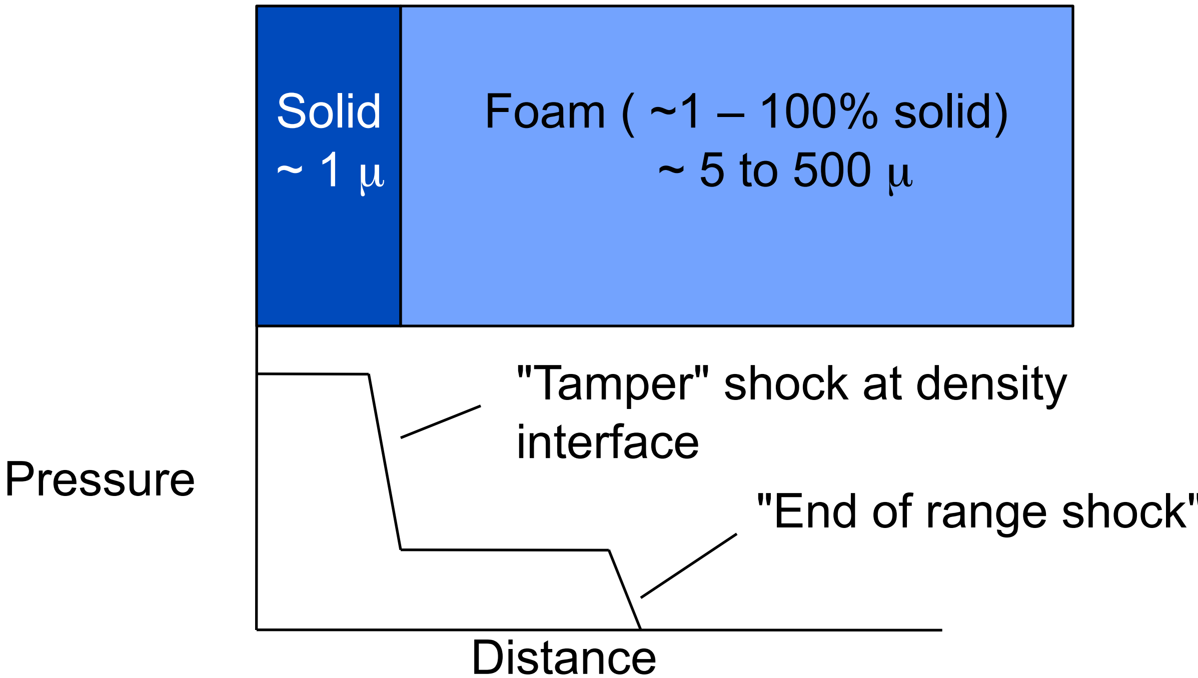

Foam examples:

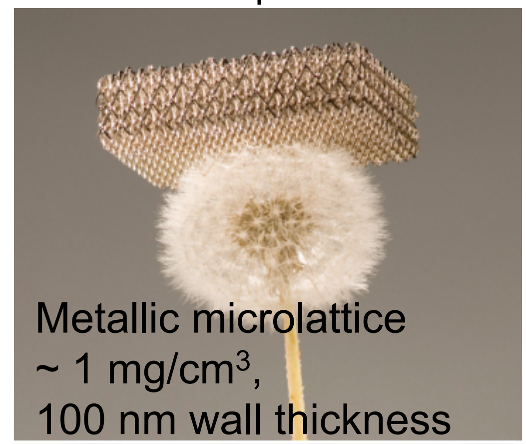

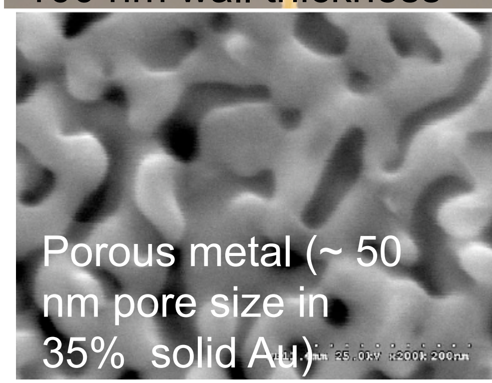

"Tamper shock" can catch up with "end of range shock"

Tamper absorbs energy that is not necessarily converted to mass flow.

What is the optimal combination of tamper thickness and density profile for efficient conversion to flow kinetic energy?

Ion stopping rates (dE/dX) in heated matter can be measured using NDCX-II both directly and indirectly

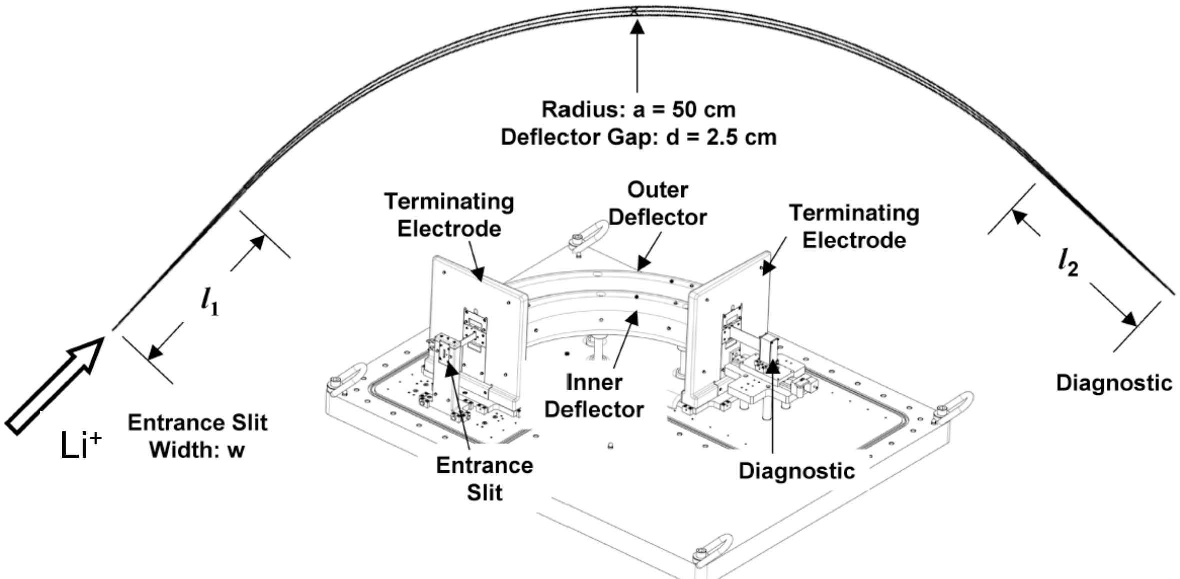

We are evaluating use of electrostatic energy analyzer (EEA) or other direct energy diagnostic for use on NDCX-II .

Indirect method: measure neutron production on deuterated carbon (plastic CD_2) target or (better) targets with known fraction of D and T.

Li+ + D → "knock-on" D (~100 kV) + D → n + charged particles

Number of created neutrons proportional to $1/(dE/dX|_{Li}) \times 1/(dE/dX|_{D})$ since the lower the dE/dX the greater chance a knock on collision will occur and the greater chance a neutron producing reaction can occur.

Conductivity in heated matter will be another area of investigation

Thermal conductivity can be measured by determining time for heat to reach various depths in foils thicker than range of ions

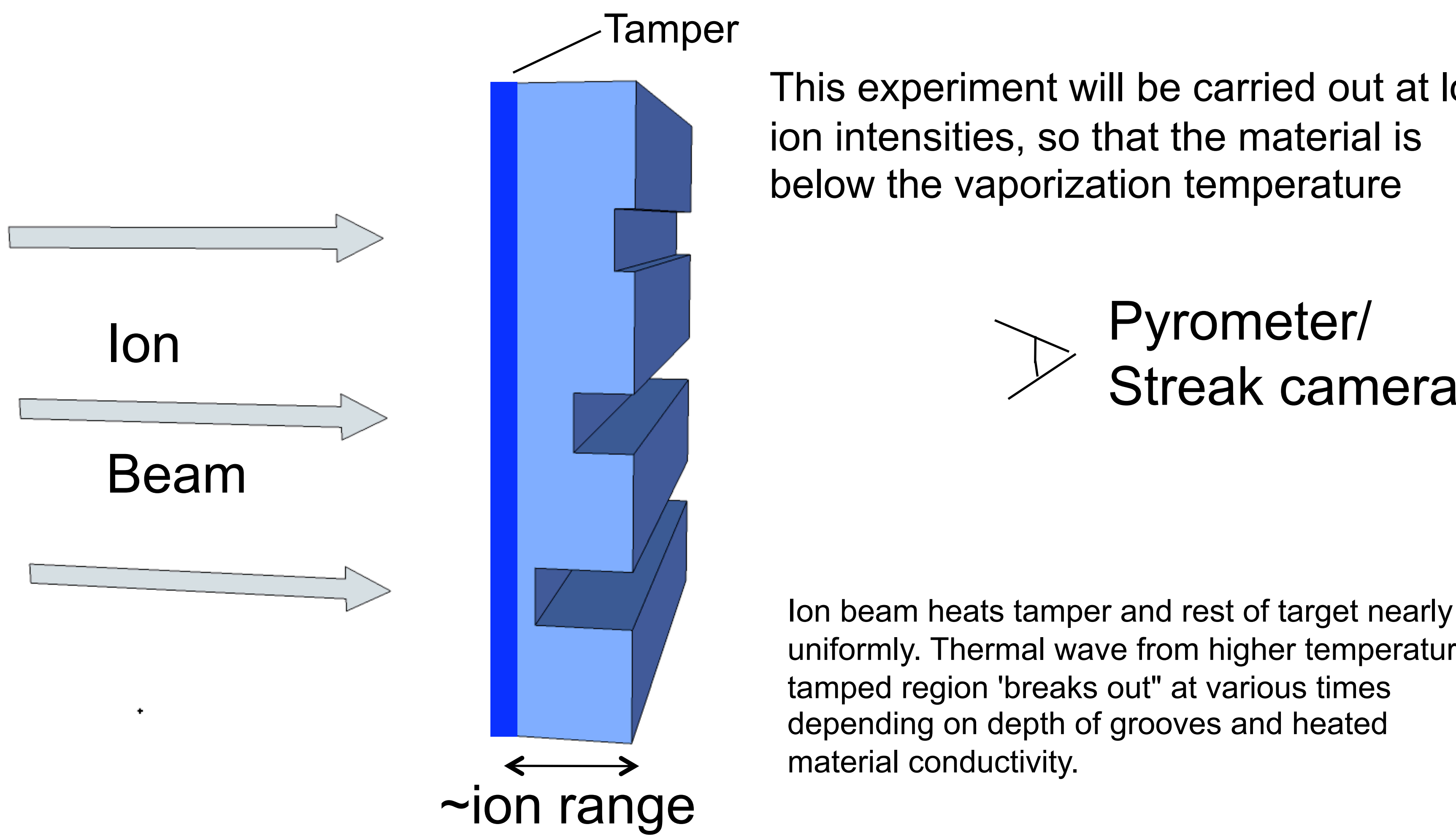

This experiment will be carried out at low ion intensities, so that the material is below the vaporization temperature

Ion beam heats tamper and rest of target nearly uniformly. Thermal wave from higher temperature tamped region 'breaks out" at various times depending on depth of grooves and heated material conductivity.

Another option: measurement of conductivity using magnetic diffusion time

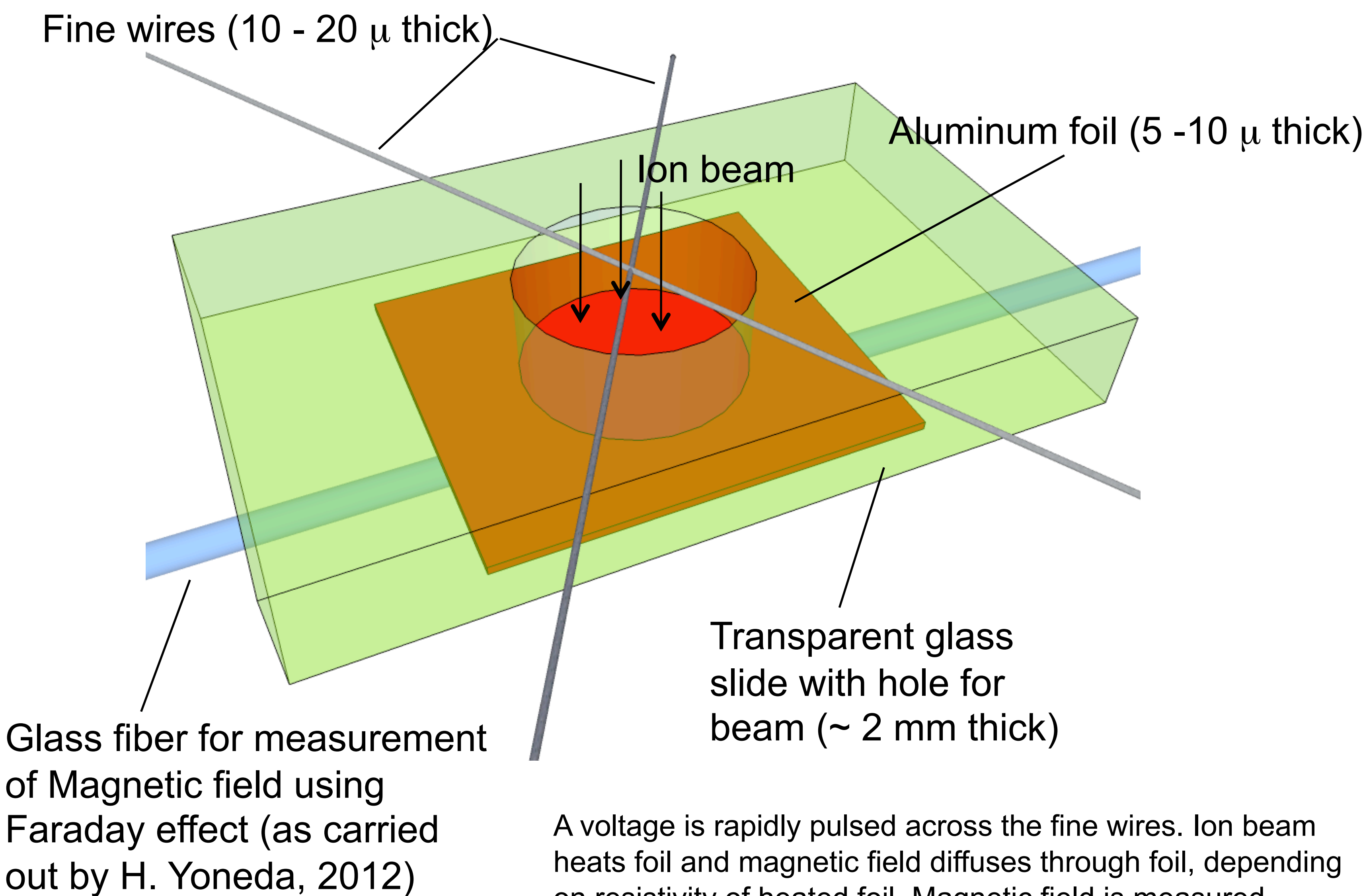

A voltage is rapidly pulsed across the fine wires. Ion beam heats foil and magnetic field diffuses through foil, depending on resistivity of heated foil. Magnetic field is measured using Faraday effect through the optical fiber.

Other areas of interest to investigators of WDM, IFE, and HIFS that may be explored in NDCX-II

1. Phase transitions: in particular liquid-vapor phase transition and the complete boundary between the regions, and critical points. (Critical point is poorly known for many of the refractory metals). (Solid-liquid phase transitions is also of interest for some material.)
2. Phase transitions from metal to insulator and insulator to metal.
3. Transition between transparent and opaque, as in transient darkening
4. Fragmentation/fracture mechanics of materials under extreme conditions (e.g. carbon, silicon)
5. Droplet formation and the role of surface tension in rapidly expanding heated metals
6. Ion beam stopping, scattering, and charge state evolution in WDM targets
7. Unusual plasma configurations, such as positive/negative plasmas (with low concentrations of electrons) as in halogens and some metals such as gold and platinum at temperatures above 0.4 eV.

Conclusions

NDCX-II will allow investigations of:

- Heavy ion fusion beam physics
- Warm dense matter target physics
- IFE relevant target physics

At 1.2 MeV we will begin to study ion beam coupling, including study of rarefaction waves to distinguish EOS models, ion based shock optimization and tamped shock physics, dE/dX measurements, and conductivity measurements

At ~3 MeV additional WDM/IFE target experiments are possible:

Ion energy exceeds Bragg peak in more material, increasing homogeneity; ion range longer, increasing hydro time; emittance scaling allows brighter beams, increasing target energy density